Soft-Landing of Peptides onto Self-Assembled Monolayer Surfaces†

Jormarie Alvarez

Department of Chemistry, Purdue University, West Lafayette, Indiana 47907

Jean H. Futrell and Julia Laskin*

Fundamental Science Directorate, Pacific Northwest National Laboratory, Richland, Washington 99352

Received: September 27, 2005; In Final Form: November 4, 2005

Mass-selected peptide ions produced by electrospray ionization were deposited as ions by soft-landing (SL) onto fluorinated and hydrogenated self-assembled monolayer (FSAM and HSAM) surfaces using a Fourier transform ion cyclotron resonance mass spectrometer (FT-ICR MS) specially designed for studying collisions of large ions with surfaces. Analysis of modified surfaces was performed in situ by combining 2 keV Cs^+ secondary ion mass spectrometry with FT-ICR detection of the sputtered ions (FT-ICR-SIMS). Similar SIMS spectra obtained following SL at different collision energies indicate that peptide fragmentation occurred in the analysis step (SIMS) rather than during ion deposition. The effect of the surface on SL was studied by comparing the efficiencies of SL on gold, FSAM, HSAM, and COOH-terminated SAM surfaces. It was found that FSAM surfaces are more efficient in retaining ions than their HSAM analogues, consistent with their larger polarizability. The efficiency of soft-landing of different peptides on the FSAM surface increases with the charge state of the ion, also consistent with an ion-polarizable molecule model for the initial stage of soft-landing on SAM surfaces. The gradual decrease of peptide ion deposition efficiency with an increase in collision energy found experimentally was quantitatively rationalized using the hard-cube model.

Introduction

Low-energy (1−100 eV) hyperthermal ion beams can be soft-landed on surfaces to modify their properties in a controlled fashion.[1,2] Collisions of low-energy ions with surfaces that result in ion soft-landing (SL) may be defined as the intact capture of mass-selected polyatomic ions at solid or liquid surfaces.[3] This process efficiently competes with scattering during the interaction of low-energy ions with semiconductive surfaces.[1,4−7] The term SL has been used to describe two distinct processes, one in which neutralization occurs during ion−surface collision and one in which the ion preserves its charge. This study is concerned with the second phenomenon. Specifically, we report here the first investigation of fundamental aspects of SL with charge retention of peptide ions on self-assembled monolayer (SAM) surfaces.

Charge retention was first demonstrated for small organic ions colliding with SAM surfaces.[8−10] Subsequent experiments utilized closed-shell organic ions,[11−14] atomic clusters,[15−18] amino acids,[19] and more recently peptides and proteins.[20−24] However, charge retention was confirmed only in a few cases.[13,14,22] Deposition of low-energy ions on liquid surfaces has been utilized to investigate the transport properties of small ions through thin films.[25,26] Oligonucleotides have been successfully soft-landed by mass spectrometry and detected by PCR.[27] Even ionized viruses have been soft-landed with retention of viability.[28] SL of mass-selected proteins has been demonstrated, and its potential application for generating protein microarrays has been described.[20] In these experiments, mass spectrometry serves as a method of separation based on physical principles that are different from and complementary to those employed in more conventional separation methods. Experimental conditions have been found under which proteins retain their biological activity during the SL experiment.[20,21]

Physical and chemical properties of the surface play a crucial role in determining the outcome of ion−surface collisions. Neutralization is a dominant process in collisions of ions with clean metal surfaces. Using thin organic films such as SAMs of thiols on metal substrates dramatically reduces neutralization and increases the efficiency of both scattering and SL of ions. The nature of the surface also strongly affects the fraction of the initial ion kinetic energy that is converted into internal energy of the impacting ion. For example, the percentage of translational-to-vibrational ($T \rightarrow V$) energy transfer is in the range 18−28% for fluorinated self-assembled monolayer (FSAM) surfaces and 12−17% for hydrogenated self-assembled monolayer (HSAM) surfaces.[29−34] For sufficiently high internal excitations, dissociation of the excited species−surface-induced dissociation (SID)−occurs.[1,34,35] The products of SID may be scattered into the gas phase or retained at the surface (crash-landing). Crash-landing has been previously reported for small polyatomic ions.[36] As noted here, FSAM surfaces efficiently convert translational energy into internal excitation of peptide ions[35,37] and competition between SL and crash-landing may present a limitation to SL efficiency.

Efficiency of SL, defined in this work as the ratio of the number of ions trapped at the surface to the number of ions colliding with the surface, is probed using secondary ion mass spectrometry (SIMS). Many factors influence SL efficiency that collectively make the interpretation of SL efficiency measure-

† Part of the special issue "William Hase Festschrift".

* Corresponding author. Present address: Fundamental Sciences Division, Pacific Northwest National Laboratory, P. O. Box 999 K8-88, Richland, WA 99352. Phone: (509)-376-4443. Fax: (509)-376-6066. E-mail: Julia.Laskin@pnl.gov.

10.1021/jp0555044 CCC: $33.50
Published on Web 12/09/2005

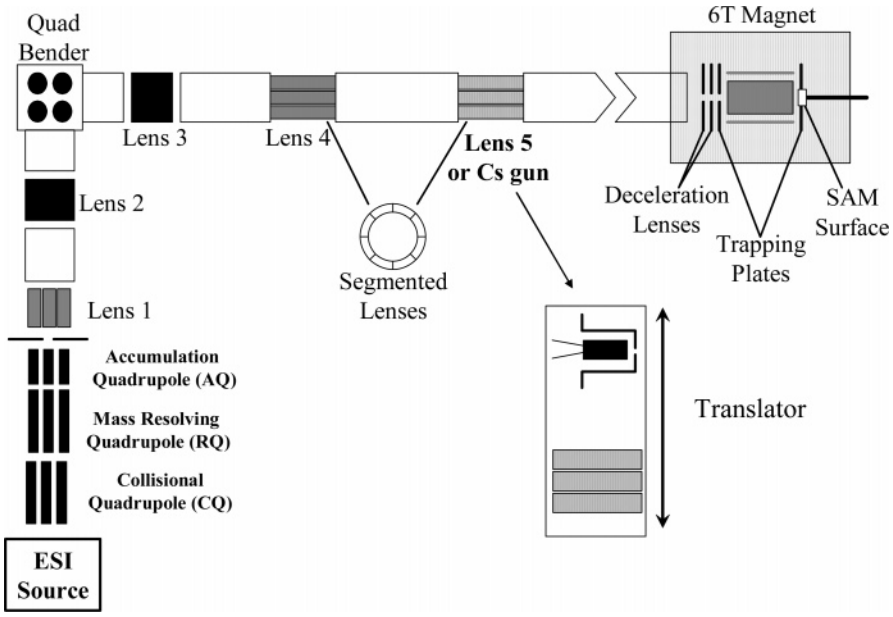

Figure 1. Schematic view of the FT-ICR mass spectrometer used for SL experiments.

ments rather difficult. SL efficiency depends on the chemical structure of the peptide, its charge state and conformation, the chemical and physical properties of the surface, and the collision energy. Neutralization by electron transfer from the SAM matrix or metal substrate decreases the desorbed ion signal and decreases the measured deposition efficiency. Sputtering and ionization of neutrals increases the apparent SL efficiency as defined here. These factors cannot be estimated within a narrow range of uncertainty.

With significant uncertainty, SL efficiencies on the order of a few percent have been estimated for small organic ions landed on FSAM surfaces.[11] Cooks and co-workers found that the SL efficiency for small organic ions maximized at a collision energy of ~10 eV where the initial kinetic energy of the ion that has to be absorbed by the surface for efficient capture is small and only a minor fraction of ions is scattered from the surface. However, difficulties in focusing low-energy ions in this study precluded quantitative investigation of the effect of collision energy on SL efficiency.[11]

Here, we report the extension of SL experiments to protonated peptides colliding with SAM (mainly FSAM and HSAM) surfaces. In our earlier systematic studies of the kinetic energy dependence of scattering of peptide ions from SAM surfaces, we found the total scattered signal for singly protonated peptides colliding with a FSAM surface increased dramatically when the collision energy was increased from 5 to 20 eV.[38,39] We suggested that capture of ions by SL might account for the low yield of scattered ions at low collision energies but did not confirm this experimentally. An even more pronounced decrease in the total scattered signal was observed for multiply protonated precursors colliding with different surfaces over a wide range of collision energies.[40] More recently, Gologan et al.[21] demonstrated charge retention by doubly protonated bradykinin on the FSAM surface. However, no systematic study has been carried out on the fate of ions remaining on the surface after collision.

The work reported here utilized a Fourier transform ion cyclotron resonance mass spectrometer (FT-ICR MS) specially configured for studying ion−surface interactions[39] combined with in situ 2 keV Cs^+ secondary ion mass spectrometry (SIMS) of modified surfaces.[22] The presence of a strong magnetic field coaxial to the ion beam allows us to manipulate the kinetic energy of the ions without defocusing.[39] This feature is essential for quantitative investigation of the influence of ion kinetic energy on SL. We investigated the dependence of SL efficiency on ion kinetic energy, the charge state of the peptide ion for FSAM and HSAM surfaces, and the kinetics of ion loss from the surface in air and high vacuum.

Experimental Section

Ionization and Deposition of Peptides Using an ESI-FT-ICR Mass Spectrometer. SL experiments were performed in a custom-built 6T FT-ICR mass spectrometer (Figure 1) described in detail elsewhere.[39] A syringe pump (Cole Parmer, Vernon Hills, IL) was used for direct infusion of the sample at a flow rate of 30 μL/h. Protonated peptides are formed in an external electrospray ionization (ESI) source and efficiently transmitted into the vacuum system using an electrodynamic ion funnel.[41] After the ion funnel, the ions undergo collisional relaxation in a collisional quadrupole (CQ) followed by mass selection using a commercial Extrel (Pittsburgh, PA) quadrupole mass filter (resolving quadrupole, RQ). Mass-selected ions are transmitted through a third quadrupole operated in the rf-only mode and pass into an electrostatic ion guide that consists of a series of five tube lenses which allow precise positioning and shaping of the ion beam. An electrostatic quadrupole bender located after the second tube lens avoids contamination of the surface by preventing neutral molecules from reaching it. After exiting the last tube lens, selected ions are transported into the ICR cell through a long flight tube. Ions are decelerated inside the strong magnetic field by two deceleration plates located at the entrance of the ICR cell.

SL occurs when mass-selected ions collide at various energies with a surface positioned at the rear trapping plate of the ICR cell. The surface is introduced through a vacuum interlock assembly and is electrically connected to the rear trapping plate of the cell. During SL experiments, static dc potentials are applied to the front trapping plate, the ring electrode, and the rear trapping plate of the ICR cell. The collision energy is defined by the difference in the potential applied to the CQ and the potential applied to the rear trapping plate and the surface. Lowering the voltage applied to the surface below ground while keeping the CQ offset fixed increases the collision energy for positive ions. Because the final kinetic energy of

the precursor ions is changed in the strong magnetic field of the ICR, ion trajectories are unperturbed by the deceleration optics.[39] Typical ion current values of about 10 pA were measured at the surface during SL experiments.

Analysis of Surfaces Using FT-ICR-SIMS. The surface was subjected to in situ Cs^+ ion desorption analysis within 5 min of completion of the ion SL experiment. The details of the FT-ICR-SIMS analysis of surfaces have been given elsewhere.[22] A Cs gun is mounted on a custom-built moving stage, which is used to interchange it with the last of the five tube lenses (lens 5) of the FT-ICR electrostatic ion guide. Primary Cs^+ ions are generated with a cesium ion gun, are transported into the ICR cell through a long flight tube, and collide with the modified surface positioned at the rear trapping plate of the ICR cell. Static SIMS conditions with a Cs^+ pulse width of 100 μs and an ion flux of about 1×10^7 ions/mm^2 per cycle (25 shots) were used in this study. Sputtered ions were captured in the ICR cell using gated trapping. Dominant Cs^+ ($m/z = 133$) and Au^+ ($m/z = 197$) ions were ejected from the ICR cell prior to the acquisition of SIMS spectra. The time elapse between the trapping event and the excitation/detection event was about 0.4 s. Data acquisition was accomplished with a MIDAS data station developed by Marshall and co-workers at the National High Magnetic Field Laboratory.[42]

Peptides. The following peptides were used for SL and subsequent analysis by FT-ICR-SIMS: singly protonated leucine enkephalin (YGGFL, *m/z* 556), angiotensin III (RVYIHPF, *m/z* 932), RVYIFPF (*m/z* 942), des-arg^1-bradykinin (PPGFSPFR, *m/z* 904), and des-arg^9-bradykinin (RPPGFSPF, *m/z* 904); doubly protonated bradykinin (RPPGFSPFR, *m/z* 530), gramicidin S (cyclo-LFPVOLFPVO, *m/z* 571), and substance P (RPKPQQFFGLM, *m/z* 674); and triply protonated renin substrate porcine (DRVYIHPFHLLVYS, *m/z* 587) and melittin (*m/z* 950). All peptides were purchased from Sigma and used as received. Samples were dissolved in a 70:30 (v/v) methanol/water solution with 1% acetic acid to a concentration of 0.1 mg/mL.

Self-Assembled Monolayer (SAM) Surfaces. Fluorinated and hydrogenated self-assembled monolayer (FSAM and HSAM) surfaces were used as targets for SL experiments. The surfaces were prepared following literature procedures.[43] In this study, $CF_3(CF_2)_9(CH_2)_2SH$ and 1-dodecanethiol were used to form the SAM by exposure of a gold surface to a 10 mM ethanol solution of the thiol for 24 h. The substrate is a silicon wafer covered with 5 nm of chromium as an adhesion layer and 200 nm of polycrystalline vapor-deposited gold (International Wafer Service, Portola Valley, CA). The surface was removed from the SAM solution, ultrasonically washed in ethanol for 5 min to remove extra layers of reagent, and dried under nitrogen gas before being introduced into the instrument.

Results

Peptide Deposition and Cs^+ Desorption. *Bradykinin (BK).* A typical FT-ICR-SIMS spectrum obtained after the deposition of doubly protonated BK, $[M + 2H]^{2+}$, on a FSAM surface is shown in Figure 2a. This experiment reports SL of 30 eV ions for 16 min using an average current of 30 pA measured at the surface. Under these conditions and with a SL spot size of 4 mm^2, the surface was exposed to a total of 9×10^{10} ions/mm^2.[44] This corresponds to about 5.4% of a monolayer assuming a cross section of 241 Å^2 for doubly protonated BK.[45,46] The spectrum shows a number of peaks characteristic of a FSAM surface such as CF_3^+, $C_2F_5^+$, Au_2F^+, $AuCF_2^+$, Au_2^+, Au_2SH^+, Au_3^+, and Au_3S^+. In addition, a peak corresponding to the singly protonated peptide, $[M + H]^+$ (*m/z* 1060), and a series of peptide fragment ions are observed. No observable intensity of doubly protonated bradykinin is found by SIMS analysis.

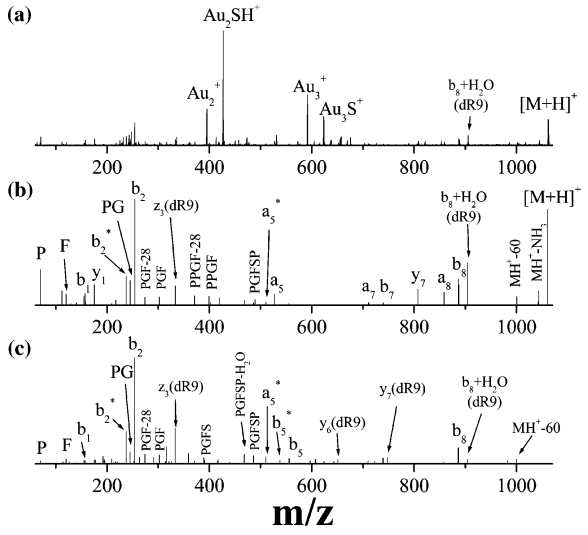

Figure 2. (a) FT-ICR-SIMS (2 keV Cs^+) spectrum of doubly charged $[M + 2H]^{2+}$ bradykinin deposited onto a FSAM surface. (b) The same spectrum without surface peaks. (c) 50 eV SID spectrum of singly protonated bradykinin on a FSAM surface.

Figure 2b repeats the 2 keV Cs^+ FT-ICR-SIMS spectrum of the FSAM surface following SL of doubly protonated BK, with characteristic surface peaks omitted for simplicity. For comparison, Figure 2c shows an SID spectrum for singly protonated BK on a FSAM surface at a collision energy of 50 eV. As discussed in prior review articles,[1,7,35,37,38] SID spectra are strongly dependent on ion kinetic energy, and this spectrum was selected from experiments obtained at different kinetic energies to illustrate the similarity of SID of singly protonated BK to SIMS analysis of doubly protonated BK soft-landed on a FSAM surface. The correspondence between the SIMS (Figure 2b) and SID (Figure 2c) spectra is striking and indicates that peptide ions excited by 50 eV collisions and ions sputtered using the 2 keV Cs^+ beam have similar internal energy distributions. A large number of backbone fragments are observed in both spectra with comparable relative abundance.

Because BK has basic arginine residues located at both termini of the peptide, fragmentation spectra contain both b-ions (b_1, b_2-NH_3, b_2, b_5, b_7, and b_8) and y-ions (y_1, y_3, y_3-NH_3, y_4-NH_3, y_6, y_7, and y_8-NH_3). In addition, internal fragments (PF, PG, PGF, PPGF PGFS, and PPGFS), immonium ions (P and F), loss of NH_3 from the singly protonated ion, and loss of 60 amu from $[M + H]^+$ characteristic of peptides containing an arginine residue at the C-terminus are all observed. The SID spectrum of bradykinin shows a number of fragment ions characteristic of des-Arg^9-bradykinin (dR9), suggesting that one of the primary fragments at *m/z* 904 is the b_8+H_2O ion, which is identical to dR9. Further fragmentation of this ion produces several characteristic fragments such as y_7 (dR9) at *m/z* 748, y_6 (dR9) at *m/z* 651, and z_3 (dR9) at *m/z* 333. This fragmentation behavior has been reported for BK by Gaskell and co-workers who proposed a rearrangement mechanism involving the loss of the C-terminal arginine to rationalize the formation of b_n+H_2O ions.[47]

Only five fragment ions observed in the FT-ICR-SIMS spectrum of soft-landed BK are not present in the Figure 2c SID spectrum. These are two a-ions (a_5 and a_7) and three y-ions (y_3, y_3-NH_3, and y_4-NH_3). Interestingly, y_3 and y_3-NH_3 are minor fragments observed in SID of doubly protonated brady-

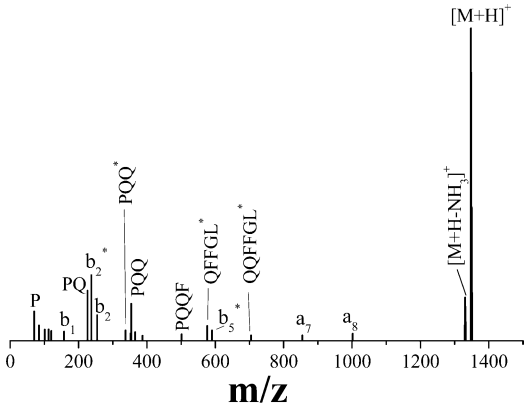

Figure 3. 2 keV Cs^+ FT-ICR-SIMS spectrum of doubly protonated $[M + 2H]^{2+}$ substance P deposited onto a FSAM surface. All of the peaks shown are fragment ions of the peptide. The peaks characteristic of the surface are omitted for simplicity. An asterisk (*) denotes loss of NH_3 from the corresponding fragment.

kinin (data not shown), while a_5 and a_7 are abundant fragments observed in high-energy collision-induced dissociation (CID) of both singly and doubly protonated BK.[48] It follows that some of the fragment ions observed in the SIMS spectra result from highly energetic dissociation pathways (possibly involving electronic excitation) that are not accessible by SID.

Substance P (SP). Figure 3 shows peptide peaks observed for substance P (RPKPQQFFGLM) analyzed using 2 keV Cs^+ FT-ICR-SIMS. In this experiment, doubly charged SP ions were deposited on a FSAM surface at a collision energy of 30 eV for 48 min and an average current of 10 pA. The ion flux of 9×10^{10} ions/mm^2 is the same as that in the previous experiment (Figure 2). Assuming that the gas-phase cross section of doubly protonated SP is 299 Å^2,[46] this corresponds to about 6.8% of a monolayer coverage. For SP, singly protonated peptide ion, $[M + H]^+$, dominates the FT-ICR-SIMS spectrum, although some fragment ions are also observed. SP exhibits significantly less fragmentation than the desorbed BK shown in Figure 2b. SID of these doubly protonated peptides at a collision energy of 30 eV demonstrated fragmentation efficiencies of about 30% for SP and 45% for BK, suggesting that BK is less stable than SP. The amount of fragmentation observed in SIMS spectra of SP and BK is correlated to their relative stability.

The SIMS spectrum of SP contains a number of b-ions (b_1, b_2, b_2-NH_3, b_3-NH_3, b_3-H_2O, b_5, and b_5-NH_3), internal fragments (PK, PQ, QQ, FFG, PQQ, $PQQ-NH_3$, $QFFG-NH_3$, and $QFFGL-NH_3$), and immonium ions (P, L, Q, F, and R). The low-mass part ($m/z < 400$) of the FT-ICR-SIMS spectrum is very similar to the 80 eV CID spectrum of the singly protonated SP reported in the literature and notably different from the CID spectrum of the doubly protonated species.[49]

Binding of Soft-Landed Peptides to the Surface. To gain insight into the nature of the interaction between the soft-landed peptide and the organic monolayer, we simply rinsed the surface with EtOH after SL and obtained the results shown in Figure 4. All of the ions corresponding to soft-landed peptide have disappeared with rinsing, while ions characteristic of the FSAM surface remain in the SIMS spectrum. This indicates that the peptide is not covalently bonded to the organic monolayer but rather adsorbed, as was found in previous studies of SL of small organic ions.[11]

Deposition Efficiency of Different Peptides. Peptides of different sizes and amino acid compositions listed in Table 1 were soft-landed on FSAM surfaces and analyzed by FT-ICR-SIMS. SIMS spectra of each of the modified surfaces showed mostly singly protonated peptide ions and some peptide fragments. It will be shown in our discussion of the desorption of soft-landed ions that they are weakly bound to the surface rather than embedded in the FSAM chains. Consequently, they are readily sputtered from the surface and sputtering yields are directly correlated to deposition efficiency. For accurate comparison of different peptides, the collision energy was kept constant at 30 eV and the total ion flux was the same for all peptides. Under these conditions, relative SL efficiency is directly related to the total peptide signal sputtered from the modified surface.

The total peptide signal (combined signal of all peaks corresponding to the deposited peptide) is a much better measure of the SL efficiency than the dominant $[M + H]^+$ signal in SIMS spectra. The fragmentation efficiency observed in SIMS spectra (see Table 1) varies dramatically with peptide composition and charge state and is not necessarily correlated to the gas-phase energetics and kinetics of dissociation of the corresponding precursors. We illustrate this by comparing the extent of fragmentation in SIMS spectra of leucine enkephalin (YGGFL) and dR1 (PPGFSPFR), peptide ions extensively studied in our laboratory using SID on the FSAM surface. SID of YGGFL results in 50% dissociation at a collision energy of ~12 eV,[50] while 27 eV is required to obtain 50% fragmentation of singly protonated dR1 on the same surface,[51] demonstrating that YGGFL is a much more fragile ion. However, 2 keV Cs^+ desorption of these peptides from the FSAM surface resulted in only 40% fragmentation of YGGFL and 60% fragmentation of the more stable dR1. Currently, we have no simple explanation for this difference.

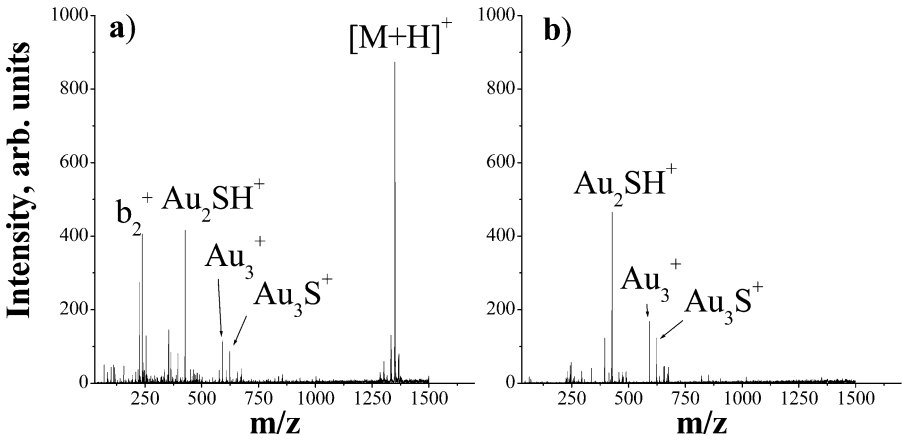

Figure 4. FT-ICR-SIMS spectrum of SP soft-landed on FSAM (a) before and (b) after rinsing the surface with ethanol.

TABLE 1: Total Peptide Signal (arb. units) and Percent Fragmentation of $[M + H]^+$ Ions Sputtered from FSAM and HSAM Surfaces after 30 eV Soft-Landing

				total peptide signal		
peptide	MW	charge state	n^a	FSAM	HSAM	AA sequence
leucine enkephalin	556.2	1	1	300 (40%)		YGGFL
des-Arg^1-bradykinin	904.4	1	2	700 (60%)		PPGFSPF***R***
des-Arg^9-bradykinin	904.4	1	2	710 (55%)		***R***PPGFSPF
angiotensin III	931.5	1	2	540 (30%)		***R***VYIHPF
RVYIFPF	941.5	1	2	630 (28%)		***R***VYIFPF
substance P	1347.7	1	4	810 (25%)		***R***P***K***PQQFFGLM$-NH_2$
renin substrate tetradecapeptide	1758.9	1	2	300 (75%)		D***R***VYIHPFHLLVYS
				average **570 ± 200**		
bradykinin	1060.5	2	3	1150 (80%)	460 (71%)	***R***PPGFSPF***R***
gramicidin S	1141	2	0	1050 (58%)	490 (65%)	LFPVOLFPVO
substance P	1347.7	2	4	1100 (42%)	560 (31%)	***R***P***K***PQQFFGLM$-NH_2$
substance P−COOH	1348.7	2	3	1500 (55%)		***R***P***K***PQQFFGLM−COOH
renin substrate tetradecapeptide	1758.9	2	2	1250 (63%)		D***R***VYIHPFHLLVYS
				average **1210 ± 180**	**500 ± 50**	

[a] *n* represents the number of free amino groups including amino groups found at the N-terminus or on the side chain of basic amino acids arginine (R) and lysine (K).

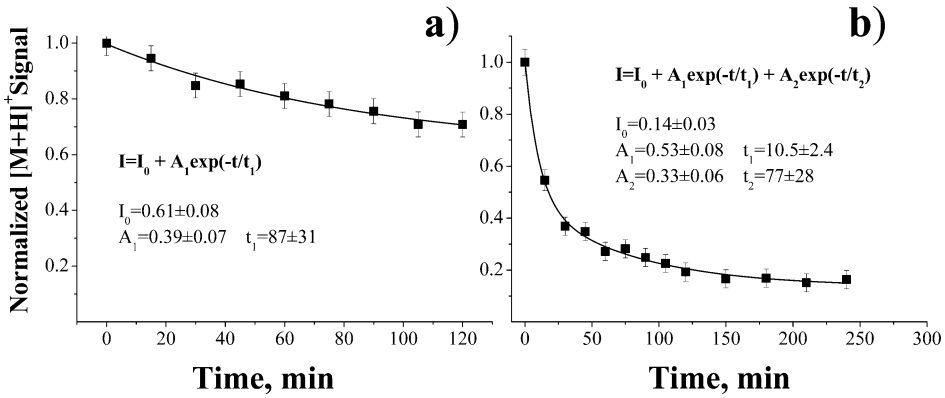

Figure 5. Loss of the total peptide signal of substance P soft-landed on a FSAM surface as a function of time (a) under vacuum (2.0×10^9 Torr) and (b) under atmospheric conditions (7.6×10^2 Torr).

Table 1 shows the total peptide signal (in arbitrary units) sputtered from FSAM surfaces modified by SL of different peptide ions under the same experimental conditions. Ion exposures of 9×10^{10} ions (<10% of a monolayer) were the same for all peptides. The values in parentheses give the relative amount of peptide fragments in SIMS spectra. The first part of the table summarizes the results obtained for singly protonated precursors, while the second part lists the data obtained for doubly protonated peptide ions. Although there are significant variations within each series of data, in most cases, they do not exceed the estimated experimental uncertainty of ~20% that results from a combination of uncertainties in ion current and surface-to-surface variations. The large uncertainty makes it impossible to correlate ion yield with more subtle factors of peptide size and structure within each data set. However, results obtained for different charge states are significantly different. The average peptide signal for singly protonated ions (570 ± 200) is 2 times smaller than the value obtained for doubly protonated precursor ions (1210 ± 180).

SL of Peptides on Different Surfaces. The relative amount of sputtered peptides was investigated after SL on FSAM, HSAM, HOOC−SAM, and gold surfaces. We found that SIMS sputtering yields of soft-landed peptides are strongly dependent on the kind of surface used for deposition. For example, angiotensin III shows a relatively high sputtering yield from FSAM surfaces; however, the sputtering yield was reduced to about 25% when the analysis was performed on a HSAM surface. Further reduction to about 4% was observed on a bare gold surface, and only about 1% relative yield was obtained by 2 keV Cs^+ bombardment of a COOH-terminated SAM surface. Table 1 shows a summary of the sputtering yields obtained for different ions soft-landed on FSAM and HSAM surfaces. The average sputtered yield is reduced by ~60% for HSAM surfaces as compared to FSAM surfaces.

Loss of Sputtered Signal Following SL. The kinetics of the loss of sputtered ion signal from the FSAM surface following SL was studied under high vacuum and atmospheric pressure. The FSAM surface was exposed to an equivalent of 25% of a monolayer of doubly protonated SP. SIMS analysis of the modified surface was performed at several delay times after the SL step. In a parallel experiment, the surface was removed from the ultrahigh vacuum (UHV) chamber (2.0×10^{-9} Torr) and exposed to laboratory air at ambient temperature for ~15 min. It was then reintroduced into the vacuum system and probed by SIMS. The experiment was repeated at several delay times to define the dependence of the total peptide signal on the time of the surface exposure to air.

The results of these two sets of experiments are shown in parts a and b of Figure 5 for the loss of ion signal with time in a vacuum and air, respectively. In a vacuum, a much smaller decrease in the peptide ion signal of about 30% was observed over a period of 2 h, while an 80% decrease in peptide signal was observed for the surface exposed to air over the same period of time.

Kinetic analysis of these two sets of experiments is quite interesting. In an UHV, 39% of the ions are involved in a slow

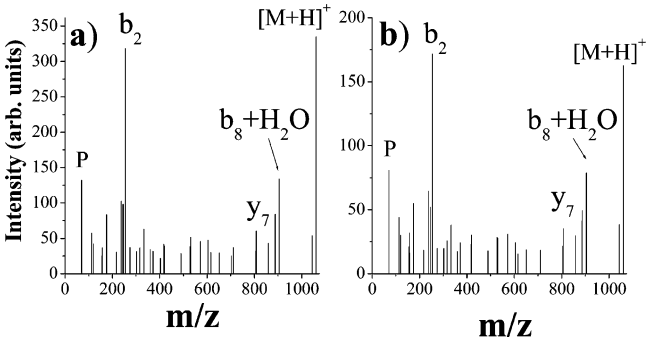

Figure 6. FT-ICR-SIMS spectrum doubly protonated BK deposited onto a FSAM surface at SL energies of (a) 10 eV and (b) 150 eV. All of the peaks shown are fragment ions of the peptide. The peaks characteristic of the surface are omitted for simplicity.

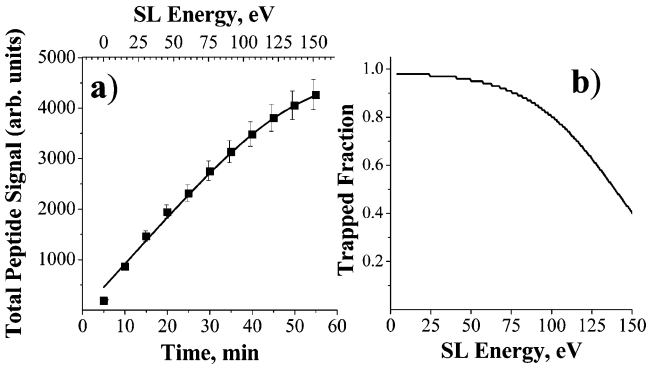

Figure 7. (a) Cumulative peptide ion abundance (bradykinin) as a function of time. The top axis shows the corresponding SL energies. The line corresponds to the hard-cube model (see text for details). (b) Trapped fraction as a function of the kinetic energy of soft-landed ions calculated using the hard-cube model.

signal loss with a lifetime of 87 ± 31 min. This strongly contrasts with the biexponential decay of peptide signal observed when the modified surface is exposed to laboratory air. In Figure 5b, about 14% of the signal shows no time dependence. The fast decay component with a lifetime of 10.5 ± 2.5 min involves ~53% of the ions, and the slow decay with a lifetime of 77 ± 28 min involves 33% of the ions.

Effect of the Collision Energy of the Peptide Ion on SL. In our experiments on peptide SL, a large number of fragments were observed in the SIMS spectra in addition to the abundant $[M + H]^+$ signal. The observed fragmentation could result from (i) crash-landing, that is, projectile ion dissociation upon impact with some of the fragments retained by the organic monolayer, or (ii) internal energy deposition onto the intact peptide (whether ion or neutral) by keV ion desorption during the SIMS analysis. These mechanisms were differentiated by SIMS analysis of surfaces modified by SL of the same peptide ion at several kinetic energies ranging from 0 to 150 eV. Figure 6 shows SIMS spectra of BK deposited onto a FSAM surface at 10 eV (Figure 6a) and at 150 eV (Figure 6b). The fraction of fragment ions formed in collision must increase as the kinetic energy of the projectile ion increases. In our experiment, a similar amount of fragmentation is observed in the SIMS spectra of the modified surfaces at both energies. Since varying the SL energy over a broad range does not affect the observed SIMS spectra, our conclusion is that peptide fragments observed in our SIMS spectra are generated during the desorption step and that crash-landing does not occur to a significant extent in these experiments.

Although no significant differences in the fragmentation pattern of deposited peptides at various SL energies were observed by SIMS analysis, the total peptide signal sputtered from the surface was a strong function of SL energy. This dependence was quantitatively investigated by exposing the surface to the ion beam and monitoring the sputtered peptide signal as the kinetic energy was varied. The SL energy was increased in 15 eV intervals from 0 to 150 eV. For each collision energy, 5 min of SL of doubly protonated BK with a measured current of 3 pA (2.8×10^9 ions per 5 min interval) was performed. This enabled the investigation of the effect of ion kinetic energy on SL efficiency using the same surface, eliminating surface-to-surface variation of the sputtered signal. This can be done as long as the total ion dose used in such experiments is well below the saturation threshold.[22] We have previously shown that the sputtered ion signal increases linearly with ion exposure as long as it does not exceed the equivalent of 30% of monolayer coverage, while at higher exposures significant deviation from linearity is observed.[22] This was attributed to saturation of surface coverage resulting from Coulomb repulsion between ions on the surface. In the present experiment, we used a low ion dose (well below the saturation threshold) to characterize ion deposition as a function of collision energy. In the entire experiment, the surface was exposed to a total of 3.1×10^{10} ions, corresponding to ~2.5% monolayer. Under these conditions, any deviation of the accumulated signal from linearity reflects the effect of collision energy on SL efficiency.

The lowest SL energy of 1 eV/charge was achieved by floating the surface at 15 V. Because ions have a distribution of kinetic energies that maximizes at a 14 V retarding potential and extends to ~20 V,[22] only 20% of the ions collide with the surface when it is floated at 15 V, while at higher collision energies all ions exiting the ion source reach the surface. Consequently, the 2 eV signal was multiplied by a factor of 5 to ensure that each point corresponds to the same ion exposure.

Total peptide signal as a function of time is shown in Figure 7a. The top axis shows the SL energy corresponding to each time point. As the collision energy increases, the total peptide signal deviates from linearity. The negative deviation shown in Figure 7a demonstrates that the SL efficiency decreases with increasing collision energy. As noted previously, a necessary prerequisite for this experiment is that ion trajectories are independent of collision energy. We have previously demonstrated that this condition is fulfilled in our experimental configuration because deceleration of the ion beam occurs inside the strong magnetic field.[38]

Discussion

Evidence for Charge Retention by Soft-Landed Peptide Ions. A central question for rationalizing our experimental data is whether peptides retain their charge following SL. Several observations from this and a previous study[22] support the hypothesis that charge is retained.

SIMS analysis of FSAM surfaces following SL of doubly protonated peptides gives mainly singly protonated species, $[M + H]^+$, and their fragments. This indicates that the peptide is partly or fully neutralized either upon impact at the surface or during the sputtering process. If the peptide ion were fully neutralized on the surface, it must then be reionized and desorbed from the surface to be detected as an ion in the SIMS spectrum. We reported previously[22] a comparison of SIMS data obtained by analyzing the same amount of substance P deposited on a FSAM surface by SL and by direct electrospray of the

neutral peptide on the surface, a standard sample preparation technique in SIMS.[52] We found a 50 times higher intensity of $[M + H]^+$ in SIMS of the SL target, indicating that soft-landed peptide ions retain their charge on the surface.[22] The increased SIMS signal results from the much higher efficiency of desorbing charged peptides relative to desorption and ionization required for SIMS analysis of neutral species.[53]

Comparison of sputtered yields obtained on different surfaces (Table 1) is also not consistent with complete neutralization of soft-landed ions. For example, if reionization of neutral peptides were necessary for obtaining a SIMS signal, one would expect higher sputtered yields from HSAMs or COOH−SAMs because sputtering from these surfaces can produce protons or small protonated molecules necessary for the formation of $[M + H]^+$ ions. However, the highest sputtered yields were obtained from FSAM surfaces and the lowest SIMS signals were observed when COOH−SAMs were used as a target. These observations strongly support the hypothesis that protonation of peptides is not a secondary reaction occurring in the sputtering process. Further support for charge retention is saturation of SIMS signal at low (<30% monolayer) surface coverage reported by us previously.[22] The signal saturation is readily rationalized as Coulomb repulsion that prevents further capture of charged ions.

Finally, comparison of the ion yields summarized in Table 1 with previous studies of sputtering yields of neutral peptides from various surfaces supports the charge retention hypothesis. For example, sputtering yields of different peptides from metallic surfaces are correlated with the number of free amino groups, *n*, at the N-terminus or in the side chain of basic amino acid residues arginine (R) and lysine (K).[54] Specifically, the yield of $[M + H]^+$ ions decreases with increasing *n*. Further, for the peptides investigated here, we find no obvious correlation between the sputtering yield and the presence of free amino groups. For example, SP ($n = 4$) has a much higher sputtering yield than leucine enkephalin or renin substrate tetradecapeptide with $n = 1$. Another example is gramicidin S (GS), for which no protonated molecular ions were produced by SIMS of the neutral sample.[54] However, in this study, we observed a very strong peak of singly protonated GS in SIMS analysis following SL. Finally, an almost exponential drop of molecular ion yields with mass reported for SIMS of neutral peptides[55] is not observed in our study. In contrast, high SIMS signals were observed for soft-landed SP, one of the largest peptides in the series.

It is very significant that *none* of the observations made for peptides electrosprayed directly into surfaces[54] correlate with our results for ions soft-landed onto surfaces. Evidently, there are major differences between these two processes of deposition. Direct electrospray onto a surface deposits neutral molecules, and ion yields observed in SIMS analysis are determined primarily by ionization and desorption efficiency for the peptide. This is readily rationalized as SIMS analysis of preformed ions on surfaces that does not require the ionization step. We conclude that peptide ions soft-landed on the FSAM surface used as a target in this study retain their charge, and ionization of the peptide is unnecessary for their detection by SIMS. We also infer that the previously reported correlation of the peptide signal in SIMS with the number of free amino groups of neutral peptides[54] reflects primarily differences in protonation efficiencies of different neutral peptides as they are sputtered from the surface.

Loss of Charge upon Soft-Landing. FT-ICR-SIMS spectra of all peptides are dominated by the $[M + H]^+$ peak. Since hardly any doubly or triply protonated peptides are observed when higher charge states of peptide ions are soft-landed, we conclude that protons are readily transferred to the surface to give the singly protonated species. This is consistent with decreasing proton affinities of peptides with the addition of each additional proton to the peptide. Close match between fragmentation patterns of soft-landed peptides observed in SIMS analysis and CID or SID of the corresponding singly protonated peptide demonstrates that a large fraction of soft-landed peptides are singly protonated species.

Crash-Landing of Peptide Ions on SAMs. Crash-landing has been previously reported for SL of $(CH_3)_3SiOSi(CH_3)_2^+$ (*m*/*z* 147) on FSAM surfaces.[11] For this molecule, the low-energy Xe^+ sputtering spectrum consisted of not only the intact parent ion but also fragment ions $(CH_3)_3Si^+$ (*m*/*z* 73), $CH_3SiH_2^+$ (*m*/*z* 45), and $C_3H_9OSi_2^+$ (*m*/*z* 117).[11] Studies at different sputtering energies confirmed that fragmentation of the deposited ion occurred upon initial ion impact and not during Xe^+ sputtering. In contrast, we have shown that crash-landing does not occur for peptide ions over a broad range of kinetic energies (Figure 6). The difference in behavior between peptide ions and small organic ions studied previously may be attributed to the large number of vibrational degrees of freedom that can effectively store the excess internal energy acquired by the peptide ion in the collision process accompanied by efficient energy transfer into the substrate prior to dissociation.

It is remarkable that intact peptide ions can be deposited on FSAM surfaces at high kinetic energies (at least up to 150 eV). This finding is especially surprising, since our previous SID studies demonstrated efficient fragmentation of peptide ions scattered off FSAM surfaces at collision energies between 20 and 60 eV.[37,38] Although SL and scattering are competing processes, our understanding of scattering and SID processes cannot be directly applied to characterize energy transfer characteristics for ions trapped on surfaces. Evidently, the ensemble of peptide ions that scatter into the gas phase and comprise the SID signal are distinctly different from the ensemble of soft-landed ions in their disposition of internal energy transferred from translation to internal energy ($T \rightarrow V$) in the collision process. A plausible interpretation is that SID ions recoil from the surface in a single repulsive collision while ions that undergo multiple collisions remain trapped on the surface and are thermalized before they have time to dissociate.

The efficiency of SL is directly correlated to the efficiency with which the kinetic energy of the precursor ion can be transferred to the surface. It is important to note that energy transfer into surface modes is very efficient for both SID and SL. In particular, we have previously demonstrated that ions scattered off the surface following energetic normal-incidence collisions have very low kinetic energies (<1 eV).[38,56] It follows that most of the initial kinetic energy of the precursor ion is redistributed into the internal modes of the ion and SAM molecules on the surface. Using the average value of $T \rightarrow V$ transfer for SID of peptide ions colliding with FSAM surfaces of 20%[37] and the negligible kinetic energy of recoiling ions, we estimate that about 80% of the initial kinetic energy of the ion is dissipated into the surface for SID ions recoiling from the surface. Energy transfer to the surface has some distribution of values, and the fraction of impacting ions that transfer more that 80% of their initial kinetic energy to the surface can remain trapped on the surface.

It is instructive to review the conclusions about energy transfer in surface collisions deduced from molecular dynamics simulations by Hase and co-workers for different but related systems. They found that on average 60% of the initial kinetic energy of

protonated triglycine is transferred to the HSAM surface for an incidence angle of 45°,[29] and ~1.6 times higher energy dissipation occurs for the normal-incidence collisions.[57] This suggests that on average some 96% of the initial kinetic energy of peptide ions can be transferred to the surface in normal-incidence collisions. A rather broad distribution of energy transfer was noted, and their results are entirely consistent with some fraction of ions being trapped by the HSAM surface and some fraction recoiling and dissociating as SID product ions.

We also note that peptide ions exhibit relatively slow unimolecular decomposition rates. Our SID studies demonstrated that peptide ions with an internal energy of less than 10 eV undergo slow statistical fragmentation.[58] For these large ions, dissociation rates are low enough that initial excitation can be dissipated into the surface before dissociation occurs. Above 10 eV internal energies, very rapid fragmentation of peptide ions occurs (shattering).[59] Onset of shattering is accompanied by a significant increase in the scattered ion signal. Because crash-landing of peptide ions is not observed in the present experiments, we conclude that most ions that acquire more than 10 eV internal energy in the collision process scatter into the gas phase and do not contribute to SL.

Factors Affecting Capture of Ions by SAM Surfaces. Capture of ions by surfaces is analyzed semiquantitatively in this section using an elaboration of the hard-cube model formalism described in detail elsewhere.[60,61] Specifically, we used the model that includes a uniform attractive potential described by Grimmelmann et al.[62] In this model, a projectile of mass M approaches the surface with velocity u and undergoes an impulsive collision with a hard cube of mass m moving with a thermal velocity distribution along the surface normal. Grimmelmann et al. derived an expression for the fraction of projectiles scattered off such a surface.[62] The nonscattered, trapped fraction can be obtained using the same formalism in a straightforward manner. The trapped fraction depends on the ratio of masses of the projectile and the hard cube, $\mu = M/m$, the kinetic energy of the projectile, the temperature of the surface, T_s, and the depth of the attractive potential, D. The solid line in Figure 7a shows the results of the hard-cube simulation for $T_s = 300$ K, in which the two variable parameters, m and D, were varied to give the best fit to the experimental data.

The best fit value of μ is 0.94 ($M = 1060$ and $m = 1130$). Values of μ obtained using this model are typically much smaller than unity and small μ's are characteristic of rigid surfaces.[61] The large value found for the FSAM surface implies that it is a soft surface, an expected result for FSAMs. The attractive well depth used in the modeling is 0.36 eV. Because the hard-cube model is rather simplistic, this value is only a very rough estimate for the well depth. However, it is clear that the trapped fraction should increase with an increase in the well depth.

Energy dependence of the calculated trapped fraction is shown in Figure 7b. The slow decrease of the trapped function at low collision energies is followed by a fairly sharp decrease at energies above 100 eV. This plot is in good qualitative agreement with data published previously for gas−surface interactions.[62] However, because the ratio of masses, μ, is close to unity, the rate of decrease of the trapped fraction with increase in collision energy is remarkably slow. As noted earlier, this is characteristic of soft surfaces. For comparison purposes, setting $\mu = 0.5$ causes the trapped fraction to decrease to zero at a 2 eV collision energy.

The efficiency of trapping and retention of ions on surfaces is determined by the attractive potential between the ion and the surface. This is given as a function of the distance, R, by the following equation:[61,63]

$$V(R) = -\frac{\alpha(eZ)^2}{2S}\int_0^\infty \frac{2\pi r\, dr}{(\sqrt{r^2+R^2})^4} = -\frac{\alpha(\pi eZ)^2}{4S}\frac{1}{R^2} \quad (1)$$

where S is the area occupied by the terminal group on the surface, e is the elementary charge, Z is the charge state of the ion, and α is the molecular polarizability of the target. Clearly, the potential well is deeper for targets with higher polarizability and for higher charge states of peptide ions. Because of the collective attraction to numerous groups on the surface, the attractive potential is a very strong function of R.

Ion Loss from the FSAM Surface. Analysis of the kinetics of the loss of sputtered signal from the surface shown in Figure 5b showed that two processes contribute to the signal loss when the surface is exposed to laboratory air: the fast decay component with a lifetime of 10.5 min and the slow decay component with a lifetime of 77 min. Because the lifetime of the slow decay component in this experiment and the lifetime determined from the UHV experiment (Figure 5a) are the same within experimental uncertainty, it is plausible to assume that the slow decay in air corresponds to the same ion loss mechanism as the one observed under vacuum.

The fast decay can be rationalized as neutralization of soft-landed ions by oxidants in laboratory air and likely involves an ion population with exposed charges. The slow decay can be attributed to desorption of physisorbed ions from the surface at room temperature. Assuming a pre-exponential factor in the range 10^9-10^{15} s^{-1} and an observed rate constant of 2×10^{-4} s^{-1}, the activation energy for desorption of ions from the surface is estimated as 20 ± 5 kcal/mol. We consider this a plausible value for physisorption of a complex charged species on the FSAM surface. Both hydrophobic interaction of the ion with the surface and ion-induced dipole interaction contribute to the binding energy of the ion to the surface. Semiempirical molecular orbital calculations demonstrated that hydrophobic interactions can be significant (~2−4 kcal/mol per interacting residue)[64] if two or more hydrophobic (alanine, phenylalanine, leucine, valine) residues are located close to the surface, while the interaction of uncharged hydrophilic residues with SAM surfaces is repulsive in nature.[65]

Equation 1 shows that ion-induced dipole interaction of the ion with the surface is a very strong function of the distance between the ion and the surface. This interaction energy is much larger when the charge is close to the surface. The charge in peptide ions is commonly located on hydrophilic residues. In particular, when basic residues (arginine, lysine, histidine) are present in the sequence, the charge is preferentially localized on these residues. It follows that the ion-induced dipole interaction is maximized when hydrophilic charge-carrying residues are oriented close to the surface. This reasoning suggests that different orientations of soft-landed ions will be preferentially bound to the surface either by hydrophobic forces or by ion-induced dipole forces. Assuming a hydrophobic binding energy of 5−7 kcal/mol, the estimated lifetime of ions on the surface at room temperature is in the range 1−200 μs, which is much shorter than the analysis time in our experiments. It follows that ions held to the surface by hydrophobic forces will escape from the surface almost instantaneously. However, the ion-induced dipole interaction can be significant. From eq 1 for the FSAM surface, an interaction energy of 20 kcal/mol is obtained at a distance of 4.6 Å for a doubly protonated ion and 2.3 Å for a singly protonated ion assuming $\alpha = 6.8 \times 10^{-24}$

cm^3 (the molecular polarizability of C_2F_6). While these arguments are admittedly qualitative, they strongly suggest that ion-induced dipole forces are an important contributor to the measured binding energy of physisorbed ions.

Effect of the Surface. Table 1 shows that FSAM surfaces are about 2 times more efficient in ion capture than their HSAM analogues. It is interesting to discuss this result in the context of our model for capture of ions by SAM surfaces. In general, molecular polarizability of hydrocarbons is about 50% lower than the polarizability of their fluorinated counterparts. However, the density of terminal CH_3 and CF_3 groups on the surface is also different. It can be estimated that the area, *S*, occupied by one methyl group is 25 $Å^2$ while the area occupied by each CF_3 group is 33 $Å^2$.[66] Consequently, according to eq 1, the attractive well between the ion and the FSAM or HSAM surfaces is very similar. By assuming the same repulsive potential for both surfaces and using eq 1 to describe the attractive potential, we estimated that the binding energy of the ion to the HSAM surface is 2−3 kcal/mol smaller than the binding energy to the FSAM surface. It is interesting to consider the effect of such a small difference on the rate of ion desorption from the surface at room temperature. Our earlier discussion established a lifetime of the order of 90 min for desorption of soft-landed ions from a FSAM surface. We estimated the binding energy for this process to be approximately 20 kcal/mol. Keeping other factors the same and decreasing this binding energy to 18 kcal/mol decreases the lifetime from 90 to 3 min. It follows from this simple argument that a large fraction of soft-landed ions are likely to escape HSAM surfaces prior to analysis.

Neutralization is another important factor that determines the effect of the surface on charge retention by soft-landed ions. Low sputtered signals obtained following SL on COOH-terminated SAM (HOOC−SAM) surfaces can be attributed to efficient neutralization of ions on the surface. The carboxylic acid terminus of the HOOC−SAM is likely solvated by water, and water molecules promote the neutralization of peptide ions, significantly reducing ion yields in SIMS analysis. In contrast, the highly inert nature of FSAM surfaces and their well-ordered structure[67−69] significantly reduces neutralization efficiency on these surfaces.

Taking all of these factors into account, we can easily rationalize the high efficiency of FSAM surfaces for soft-landing of ions and retaining them in a physisorbed state over periods of minutes to hours in high vacuum.

Conclusions

This work presented the first systematic study of several factors that affect soft-landing of peptide ions on SAM surfaces. We deposited peptide ions of different compositions and charge states on SAM surfaces followed by the in situ analysis of modified surfaces using 2 keV Cs^+ SIMS inside the FT-ICR mass spectrometer used for SL. Peptide ions are particularly attractive model systems that provide important insights on the behavior of soft-landed proteins. Fundamental principles derived from such studies of interaction of protonated peptides with hydrophobic surfaces are relevant to the transport of biomolecules through membranes in living organisms.

We presented evidence that peptide ions retain at least one proton after SL on FSAM or HSAM surfaces. Because this eliminates the inefficient ionization step in SIMS analysis of modified surfaces, very large ion yields are observed in FT-ICR-SIMS spectra. Special characteristics of our FT-ICR apparatus enabled quantitative investigation of the effect of the initial kinetic energy of peptide ions on SL. We found that in the range of collision energies from 0 to 150 eV SL deposits intact ions on surfaces. In contrast with previous studies that demonstrated crash-landing of organic ions at higher collision energies, we found that peptide fragments observed in SIMS spectra at all collision energies were produced in the analysis step and not during ion SL.

Most of our findings can be rationalized using the hard-cube model. For example, the decrease of the SL efficiency with an increase in collision energy is well reproduced using this model. The lower SL efficiency on the HSAM surface can be attributed to somewhat weaker binding of ions to the surface with lower polarizability, while the slow decay of the sputtered signal with time can be rationalized as a slow physisorption of ions from a potential well of ∼20 kcal/mol dominated by electrostatic forces. We suggest that ions are oriented with their charged residues to the surface to maximize their binding energy and that ion loss involves rotation of the ion on the surface that results in larger separation distances and weakens the ion−surface interaction. The larger SL efficiencies observed for doubly protonated ions as compared to singly protonated ions are in good agreement with this model.

Acknowledgment. We thank Prof. Graham Cooks for very insightful discussions of different aspects of this project and critical reading of the manuscript. We also gratefully acknowledge helpful discussions with Dr. S. E. Barlow and Professors Raphael Levine and William Hase. The research described in this manuscript was performed at the W. R. Wiley Environmental Molecular Sciences Laboratory (EMSL), a national scientific user facility sponsored by the U.S. Department of Energy's Office of Biological and Environmental Research and located at Pacific Northwest National Laboratory (PNNL). PNNL is operated by Battelle for the U.S. Department of Energy. Research at EMSL was supported by the grant from the Chemical Sciences Division, Office of Basic Energy Sciences of the U.S. Department of Energy. Research at Purdue University was supported by the National Science Foundation (CHE 0412782). J.A. acknowledges participation in the PNNL Interfacial and Condensed Phase Summer Research Institute.

References and Notes

(1) Grill, V.; Shen, J.; Evans, C.; Cooks, R. G. *Rev. Sci. Instrum.* **2001**, *72*, 3149−3179.
(2) Hanley, L.; Sinnott, S. B. *Surf. Sci.* **2002**, *500*, 500.
(3) Gologan, B.; Green, J. R.; Alvarez, J.; Laskin, J.; Cooks, R. G. *Phys. Chem. Chem. Phys.* **2005**, *7*, 1490.
(4) Kasi, S. R.; Kang, H.; Sass, C. S.; Rabalais, J. W. *Surf. Sci. Rep.* **1989**, *10*, 1.
(5) Jacobs, D. C. *Annu. Rev. Phys. Chem.* **2002**, *53*, 379.
(6) Cooks, R. G.; Ast, T.; Mabud, A. *Int. J. Mass Spectrom. Ion Processes* **1990**, *100*, 209−265.
(7) Dongre, A. R.; Somogyi, Á.; Wysocki, V. H. *J. Mass Spectrom.* **1996**, *31*, 339−350.
(8) Franchetti, V.; Solka, B. H.; Baitinger, W. E.; Amy, J. W.; Cooks, R. G. *Int. J. Mass Spectrom. Ion Processes* **1977**, *23*, 29.
(9) LaPack, M. A.; Pachuta, S. J.; Busch, K. L.; Cooks, R. G. *Int. J. Mass Spectrom. Ion Phys.* **1983**, *53*, 323.
(10) Miller, S. A.; Luo, H.; Pachuta, S.; Cooks, R. G. *Science* **1997**, *275*, 1447.
(11) Luo, H.; Miller, S. A.; Cooks, R. G.; Pachuta, S. J. *Int. J. Mass Spectrom.* **1998**, *174*, 193.
(12) Shen, J.; Yim, Y. H.; Feng, B.; Grill, V.; Evans, C.; Cooks, R. G. *Int. J. Mass Spectrom.* **1999**, *183*, 423.
(13) Cooks, R. G.; Ast, T.; Mabud, M. A. *Int. J. Mass Spectrom. Ion Processes* **1990**, *100*, 209.
(14) Schultz, D. G.; Lim, H.; Garbis, S.; Hanley, L. *J. Mass Spectrom.* **1999**, *34*, 217.
(15) Kaiser, B.; Bernhardt, T. M.; Stegemann, B.; Opitz, J.; Rademann, K. *Phys. Rev. Lett.* **1999**, *83*, 2918−2921.

(16) Messerli, S.; Schintke, S.; Morgenstern, K.; Sanchez, A.; Heiz, U.; Schneider, W. D. *Surf. Sci.* **2000**, *46*, 331.
(17) Yamaguchi, W.; Yoshimura, K.; Tai, Y.; Maruyama, Y.; Igarashi, K.; Tanemura, S.; Murakami, J. *Chem. Phys. Lett*. **1999**, *311*, 341.
(18) Palmer, R. E.; Pratontep, S.; Boyen, H. G. *Nat. Mater*. **2003**, *2*, 443.
(19) Nanita, S. C.; Takats, Z.; Cooks, R. G. *J. Am. Soc. Mass Spectrom.* **2004**, *15*, 1360.
(20) Ouyang, Z.; Takats, T. A.; Blake, B.; Gologan, A. J.; Guymon, J. M.; Wiseman, J. C.; Oliver, V. J.; Davisson, Cooks, R. G. *Science* **2003**, *301*, 1351.
(21) Gologan, B.; Takáts, Z.; Alvarez, J.; Wiseman, J. M.; Talaty, N.; Ouyang, Z.; Cooks, R. G. *J. Am. Soc. Mass Spectrom*. **2004**, *15*, 1874.
(22) Alvarez, J.; Cooks, R. G.; Barlow, S. E.; Gaspar, D. J.; Futrell, J. H.; Laskin, J. *Anal. Chem.* **2005**, *77*, 3452.
(23) Volny, M.; Elam, W. T.; Ratner, B. D.; Turecek, F. *Anal. Chem.* **2005**, *77*, 4846.
(24) Volny, M.; Elam, W. T.; Branca, A.; Ratner, B. D.; Turecek, F. *Anal. Chem.* **2005**, *77*, 4890.
(25) Cowin, J. P.; Tsekouras, A. A.; Iedema, M. J.; Wu, K.; Ellison, G. B. *Nature* **1999**, *398*, 405.
(26) Tsekouras, A. A.; Iedema, M. J.; Cowin, J. P. *J. Chem Phys.* **1999**, *111*, 2222.
(27) Feng, B.; Wunschel, D. S.; Masselon, C. D.; Pasa-Tolic, L.; Smith, R. D. *J. Am. Chem. Soc.* **1999**, *121*, 8961.
(28) Siuzdak, G.; Bothner, B.; Yeager, M.; Brugidou, C.; Fauquet, C. M.; Hoey, K.; Chang, C. M. *Chem. Biol.* **1996**, *3*, 45.
(29) Meroueh, O.; Hase, W. L. *J. Am. Chem. Soc*. **2002**, *124*, 1524.
(30) Morris, M. R.; Riederer, D. E. J.; Winger, B. E.; Cooks, R. G.; Ast, T.; Chidsey, C. E. D. *Int. J. Mass Spectrom. Ion Processes* **1992**, *122*, 181.
(31) Cooks, R. G.; Ast, T.; Mabud, M. A. *Int. J. Mass Spectrom. Ion Processes* **1990**, *100*, 209.
(32) Schultz, D. G.; Lim, H.; Garbis, S.; Hanley, L. *J. Mass Spectrom.* **1999**, *34*, 217.
(33) Laskin, J.; Futrell, J. H. *J. Chem. Phys.* **2003**, *119*, 3413.
(34) Vekey, K.; Somogyi, A.; Wysocki, V. H. *J. Mass Spectrom.* **1995**, *30*, 212.
(35) Laskin, J.; Futrell, J. H. *Mass Spectrom. Rev.* **2003**, *22*, 158.
(36) Shen, J.; Yim, Y. H.; Feng, B.; Grill, V.; Evans, C.; Cooks, R. G. *Int. J. Mass Spectrom.* **1999**, *182/183*, 423.
(37) Laskin, J.; Futrell, J. H. *J. Am. Soc. Mass Spectrom.* **2003**, *14*, 1340.
(38) Laskin, J.; Futrell, J. H. *Mass Spectrom. Rev.* **2005**, *24*, 135.
(39) Laskin, J.; Denisov, E. V.; Shukla, A. K.; Barlow, S. E.; Futrell, J. H. *Anal. Chem.* **2002**, *74*, 3255.
(40) Laskin, J. Unpublished results.
(41) Shaffer, S. A.; Tang, K.; Anderson, G. A.; Udseth, H. R.; Smith, R. D. *Rapid Commun. Mass Spectrom.* **1997**, *11*, 1813−1817.
(42) Senko, M. W.; Canterbury, J. D.; Guan, S.; Marshall, A. G. *Rapid Commun. Mass Spectrom.* **1996**, *10*, 1839.
(43) Chidsey, C.; Liu, G.; Rowntree, P.; Scoles, G. *J. Chem. Phys.* **1989**, *91*, 4421.
(44) Under these experimental conditions, the maximum potential resulting from the accumulation of an electrical charge on the surface is 0.2 V, assuming that all ions retain their charge.
(45) Wyttenbach, T.; Helden, G. V.; Bowers, M. T. *J. Am. Chem. Soc.* **1996**, *118*, 8355.
(46) Gill, A. C.; Jennings, K. R.; Wyttenbach, T.; Bowers, M. T. *Int. J. Mass Spectrom.* **2000**, *195*−*196*, 685.
(47) Thorne, G. C.; Ballard, K. D.; Gaskell, S. J. *J. Am. Soc. Mass Spectrom.* **1990**, *1*, 249−257.
(48) Nielsen, S. B.; Andersen, J. U.; Hvelplund, P.; Jorgensen, T. J. D.; Sorensen, M.; Tomita, S. *Int. J. Mass Spectrom.* **2002**, *213*, 225.
(49) Qin, X.-Z.; Yuan, Y. *Int. J. Mass Spectrom.* **2004**, *237*, 123.
(50) Laskin, J. Unpublished results.
(51) Laskin, J.; Bailey, T. H.; Denisov, E. V.; Futrell, J. H. *J. Phys. Chem. A* **2002**, *106*, 9832.
(52) McNeal, C. J.; Macfarlane, R. D.; Thurston, E. L. *Anal. Chem.* **1979**, *51*, 2036.
(53) Busch, K. L.; Unger, S. E.; Vincze, A.; Cooks, R. G.; Keough, T. *J. Am. Chem. Soc*. **1982**, *104*, 1507.
(54) Benninghoven, A.; Rudenauer, F. G.; Werner, H. W. *Secondary Ion Mass Spectrometry: Basic Concepts, Instrumental Aspects, Applications and Trends*, *Chemical Analysis*; Series of Monographs on Analytical Chemistry and Its Applications, Vol. 86; Wiley: New York, 1987.
(55) Ens, W.; Beavis, R.; Main, D.; Tang, X.; Chait, B. T. Presented at the 34th ASMS Conference on Mass Spectrometry and Allied Topics, Cincinnati, OH, 1986.
(56) Rakov, V. S.; Futrell, J. H.; Denisov, E. V.; Nikolaev, E. N. *Eur. J. Mass Spectrom.* **2000**, *6*, 299.
(57) Wang, J.; Meroueh, O.; Wang, Y.; Hase, W. L. *Int. J. Mass Spectrom.* **2003**, *230*, 57.
(58) Laskin, J. *Eur. J. Mass Spectrom*. **2004**, *10*, 259.
(59) Laskin, J.; Bailey, T. H.; Futrell, J. H. *J. Am. Chem. Soc.* **2003**, *125*, 1625.
(60) Logan, R. M.; Stickney, R. E. *J. Chem. Phys.* **1966**, *44*, 195.
(61) Levine, R. D. *Molecular Reaction Dynamics*; Cambridge University Press: Cambridge, U.K., 2005.
(62) Grimmelmann, E. K.; Tully, J. C.; Cardillo, M. J. *J. Chem. Phys.* **1980**, *72*, 1039.
(63) Levine, R. D. Private communication.
(64) Latour, R. A.; Rini, C. J. *J. Biomed. Mater. Res.* **2002**, *60*, 564.
(65) Latour, R. A.; Hench, L. L. *Biomaterials* **2002**, *23*, 4633.
(66) Alves, C. A.; Porter, M. D. *Langmuir* **1993**, *9*, 3507.
(67) Chidsey, C. E. D.; Loiacono, D. M. *Langmuir* **1990**, *6*, 682.
(68) Miura, Y. F.; Takenaga, M.; Koini, T.; Graupe, M.; Garg, N.; Graham, R. L., Jr.; Lee, T. R. *Langmuir* **1998**, *14*, 5821.
(69) Whitesides, G. M.; Laibinis, P. E. *Langmuir* **1990**, *6*, 87.